
Superresolution Source Location with Planar Arrays

Gary F. Hatke

■ The challenge of precision source location with a radio-frequency antenna array has existed from the beginnings of radiometry and has continued in modern applications with planar antenna arrays. Early work in this field was limited to estimating single source directions in one dimension with systems like crossed-loop radiometers. Currently, more advanced systems attempt to estimate azimuth and elevation by using two-dimensional arrays. Monopulse techniques have been extended to two-dimensional arrays to provide a computationally efficient method for estimating the azimuth and elevation of a single source from a planar array, but all monopulse techniques fail if there is appreciable interference close to the source. In this situation, adaptive array (superresolution) processing techniques are needed for direction estimation.

This article discusses the results of a study on the proper way to design an adaptive planar array with a constrained antenna aperture. We consider the segmentation of the antenna aperture, the polarization of the antenna segments, and the algorithms used to process the signals received from the antenna. In particular, we concentrate on interference that is within one Rayleigh beamwidth of the source. The interference can be highly localized in space, as in a single direct-path interferer, or diffuse in space (possibly due to multipath). We present results of tests conducted with a segmented antenna array, along with simulations and analytical bounds, that guide us in designing a source-location system.

ESTIMATING THE LOCATION of a source in the presence of interference is a complex challenge for a direction-finding system. Most traditional direction-finding systems are designed with a monopulse antenna-array configuration that segments the antenna array into four symmetrical subapertures, as shown in Figure 1. This array configuration, or topology, allows estimating both azimuth and elevation of the source.

In nonadaptive direction-finding systems, the antenna patterns of the subapertures are designed to suppress most interference from outside the main beam of the array. When the interference is inside the main beam of the array—by definition closer (in radians) to the source than the inverse (in wavelengths) of the direction-finding antenna-array aperture—a non-

adaptive technique cannot suppress the interference. Traditionally, radar designers have solved this problem by increasing the aperture of the antenna array until the interference is no longer inside the main beam. This solution can be impossible to implement, however, if the array is physically constrained and the wavelength of the radiation cannot be changed. In this case, adaptive array (superresolution) processing techniques must be employed to accurately estimate the source location.

Two approaches for source-location estimates with main-beam interference can be used, depending on whether the interference is pointlike or diffuse. For simplicity, we assume that there is only one interferer in the main beam. If the main-beam interference is caused by a pointlike interferer, conventional mono-

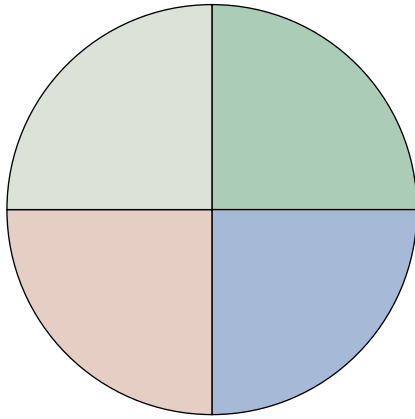


FIGURE 1. Four-subaperture circular array. This configuration allows estimation of source azimuth and elevation.

pulse antenna topology and superresolution algorithms may be applied to the data from the four subapertures of the array to suppress the interference. Problems arise when the main-beam interference is diffuse as a result of incoherent multipath scattering of the interference. In this case, applying adaptive techniques to a conventional quadrant array may not suppress the diffuse interference in the main beam of the array. This limitation also applies if there are multiple main-beam interferers. Again, for simplicity, we concentrate on the single interferer case.

To suppress diffuse main-beam interference effectively, we can divide the array into more subapertures than the conventional four. This additional segmentation gives more channels of information, hence more degrees of freedom, to the adaptive-array processing algorithm, allowing improved interference suppression. We can also increase the degrees of freedom by receiving two different polarizations from some or all of the array subapertures. This strategy is useful when the interference and source have different polarization states. These approaches to suppress main-beam interference come at a price—each additional channel from the array requires an additional receiver, and the complexity of the adaptive-array processing algorithms that process the multichannel data increases in proportion to the cube (or higher) of the number of data channels.

We conducted a two-part study to explore the best combinations of array topologies and superresolution algorithms that accurately estimate source location.

First, we studied the minimum required segmentation to allow an adaptive-array processing algorithm to accurately estimate the direction of a source in the presence of either diffuse or pointlike main-beam interference. Results of this study indicate that for planar arrays, more than four subapertures are desirable when diffuse main-beam interference is present. We also found that using nonidentically polarized subapertures can be beneficial when the interference has a relatively pure polarization that differs from the source.

We then developed computationally efficient algorithms that could be coupled with a wide range of array-segmentation topologies to give nearly optimal estimates of source direction. The new algorithms are called PRIME (polynomial root intersection for multidimensional estimation) and GAMMA (generalized adaptive multidimensional monopulse algorithm). These algorithms have been shown through simulation and analytical derivations to have estimate variances that equal previous state-of-the-art algorithms at a fraction of the computational cost. We use GAMMA when we have an estimate of the spatial covariance matrix (the spatial power distribution) of the interference signal in the absence of the desired source signal. We use PRIME when we cannot get desired source-free observations of the spatial power distribution. Both algorithms are multidimensional generalizations of previously proposed one-dimensional rooting algorithms that convert the direction-estimation task to one of finding roots to a polynomial equation.

We verified the performance of the selected antenna-array topology designs and the adaptive-array processing algorithms by using a segmented antenna array. Source directions were successfully estimated by using both the PRIME and GAMMA algorithms in the presence of either diffuse main-beam interference or pointlike main-beam interference.

Planar-Array Primer

Because estimating the direction to a source is a two-dimensional problem, two angles must be estimated per source, which requires at least a two-dimensional array. Figure 2 shows the simplest array topology that meets this requirement—a three-subaperture planar array. While this array topology allows the simulta-

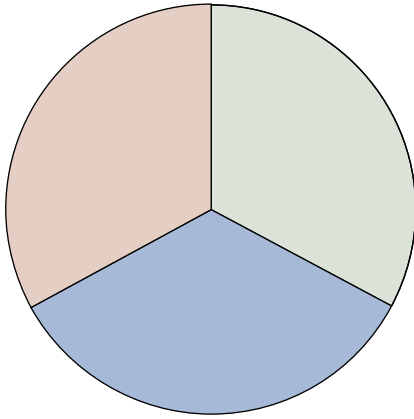


FIGURE 2. Three-subaperture circular array. This configuration is the simplest array topology that allows estimation of source elevation and azimuth angles.

neous estimation of elevation and azimuth angles, an array topology with four subapertures arranged as in Figure 1 can be transformed into a three-channel array via a unitary beamforming matrix to provide estimates of elevation and azimuth angles for a source signal. The three-subaperture array has no such simple method for producing source-angle estimates, and therefore is rarely used. The three-channel (from four subapertures) system is often called a monopulse system, because it was originally designed to estimate a desired source's azimuth and elevation by using a single pulse from a pulsed radar.

To see how this transformation occurs, let us look at the output of the four-subaperture array in the absence of noise, with a desired signal waveform $s(t)$ at an azimuth θ and an elevation ϕ . The array output vector $\mathbf{x}(t)$ has the form

$$\mathbf{x}(t) = s(t) \begin{bmatrix} e^{jk(u_1+u_2)} \\ e^{jk(u_1-u_2)} \\ e^{-jk(u_1+u_2)} \\ e^{-jk(u_1-u_2)} \end{bmatrix}. \quad (1)$$

Here we define an array constant k as $2\pi d/\lambda$, where d is the distance from the center of the array to the effective phase center of one of the quadrants, and λ is the wavelength of the center frequency of the radio-frequency (RF) signal. The array constant k , which varies inversely with the array beamwidth, can be

thought of as a scaled distance between the array phase reference (here taken to be the center of the array) and the phase center of a given subaperture. The terms u_1 and u_2 are functions of the azimuth and elevation of the desired source:

$$\begin{aligned} u_1 &= \sin \theta \\ u_2 &= \cos \theta \sin \phi. \end{aligned}$$

The monopulse beamforming network can be mathematically represented by a 4×4 matrix \mathbf{M} :

$$\mathbf{M} = \frac{1}{4} \begin{bmatrix} 1 & 1 & 1 & 1 \\ j & j & -j & -j \\ j & -j & -j & j \\ -1 & 1 & -1 & 1 \end{bmatrix}.$$

The output $\mathbf{y}(t)$, after applying the beamforming network, is a vector of four beams with the form

$$\mathbf{a}s(t) = \mathbf{y}(t) = \mathbf{M}\mathbf{x}(t) = \begin{bmatrix} \cos(ku_1) \cos(ku_2) \\ \sin(ku_1) \cos(ku_2) \\ \cos(ku_1) \sin(ku_2) \\ \sin(ku_1) \sin(ku_2) \end{bmatrix} s(t).$$

An estimate for u_1 is the arctangent of the voltage ratio of the second beam $[\sin(ku_1) \cos(ku_2)s(t)]$ to the first beam $[\cos(ku_1) \cos(ku_2)s(t)]$ divided by the array constant k , and an estimate of u_2 is the similarly scaled arctangent of the voltage ratio of the third beam $[\cos(ku_1) \sin(ku_2)s(t)]$ to the first beam. The array-response vector \mathbf{a} after the monopulse transformation is real for all values of u_1 and u_2 because of the centrosymmetric nature of the four-subaperture square antenna array. A centrosymmetric array is one with a phase center such that all subapertures in the array appear in pairs around the phase center. Centrosymmetric arrays are useful topologies because there is always a beamforming matrix that produces array-response vectors that are entirely real.

Three-channel systems do well in estimating single source directions when the array receives no interference. However, if one or more of the three beams used for direction estimation in a monopulse system

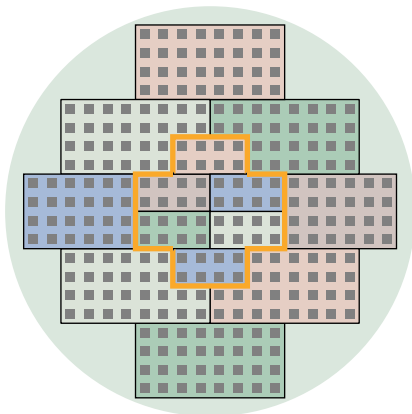


FIGURE 3. Sampled aperture sensor (SAS) subaperture configurations. The SAS was designed with an eight-subaperture sixteen-channel large outer array, which allows a wide range of aperture and array configuration trade-offs, and a smaller, six-subaperture twelve-channel inner array.

receive an interference signal, the resulting angle estimates are corrupted. Because of the limited degrees of freedom in a three-channel monopulse system, even if the outputs are combined adaptively it is impossible to eliminate the effects of the interference from the desired source-angle estimates. For this reason, all centrosymmetric adaptive planar-array processing systems have four or more antennas with at least four independent channels at the output of any beamformer. When an interference environment consists of more than a single point source in the main beam, such as diffuse multipath or multiple point-source interference, then even a four-channel system is unable to cope with the interference environment. This limitation implies that an antenna-segmentation topology with more than four subapertures will be beneficial.

Array-Topology Study

Lincoln Laboratory studied the benefits of alternate antenna segmentation topologies while attempting to track a source with diffuse interference within one array beamwidth of the source. A multi-aperture array, known as the sampled aperture sensor (SAS), was constructed with fourteen dual-polarized subapertures, giving twenty-eight possible outputs. The SAS was designed with an eight-subaperture sixteen-channel large outer array, which gave us a larger array aper-

ture and allowed a larger number of array configurations, and a smaller, six-subaperture twelve-channel inner array, as shown in Figure 3. The outer eight-subaperture array has an effective beamwidth of six degrees; the inner six-subaperture array has an effective beamwidth of sixteen degrees. Because of limited receiver resources, only eight subapertures could be used simultaneously. Thus we constructed a switching system that allowed the array operator to choose from five configurations of eight subapertures. Figure 4 shows the dual-polarized patch SAS array. Each subaperture has roughly 25 to 30 dB of polarization isolation between the vertical and horizontal outputs.

To achieve desired source-angle estimates in the presence of main-beam interference, the SAS must be well calibrated [1]. We performed a pattern response equalization for spatial similarity (PRESS) array cali-

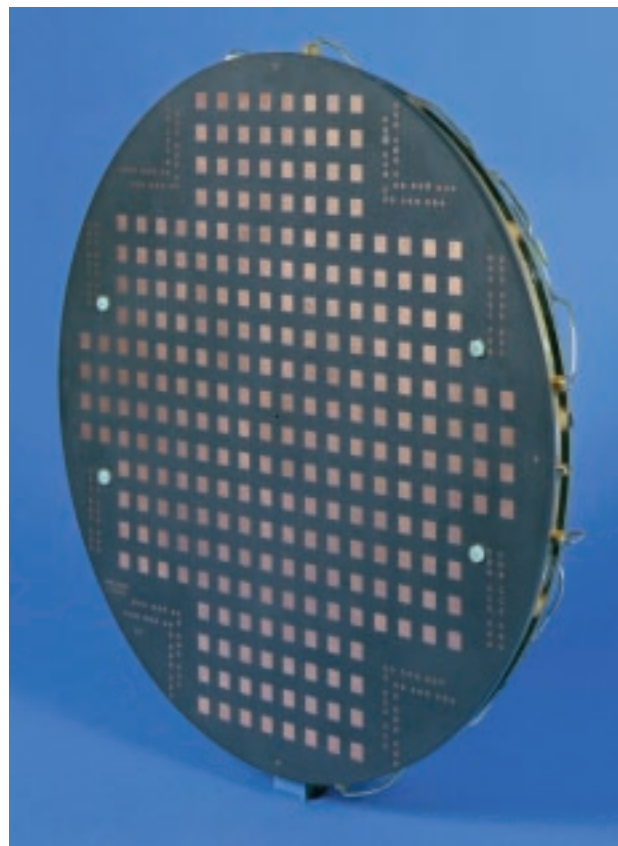


FIGURE 4. Sampled aperture sensor. The outer eight-aperture array has an effective beamwidth of six degrees; the inner six-aperture array has an effective beamwidth of sixteen degrees. Both arrays are dual-polarized with patch-antenna technology.

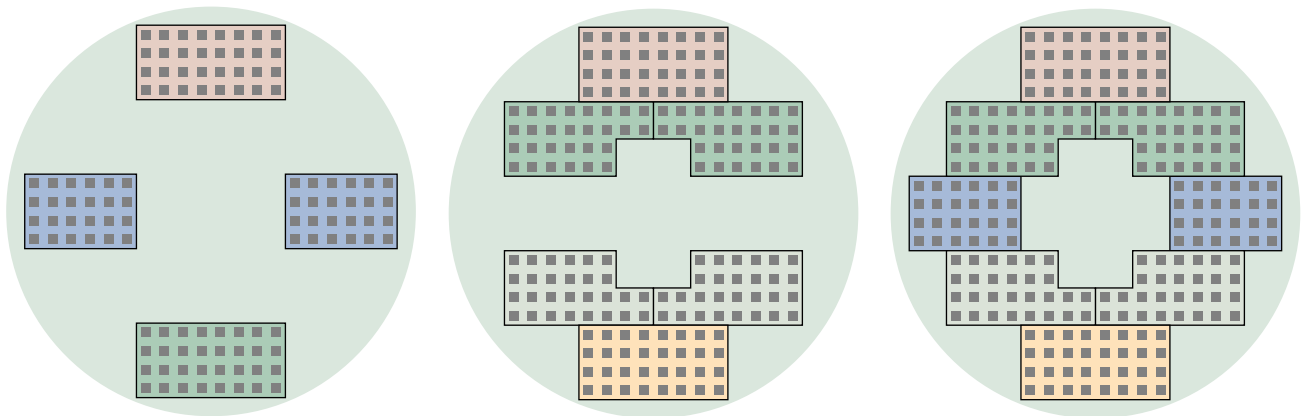


FIGURE 5. Examples of SAS array configurations. Arrays of three, four, and five distinct vertical subapertures were simulated by analyzing data from different subsets of the available eight channels.

bration of the SAS mounted with its receivers. The calibration-error residual is defined as the average length of the difference vector between the assumed array response (normalized to length of one) and the properly normalized array response from the PRESS algorithm. The average calibration-error residual is taken over all azimuths and elevations for which the calibration is expected to be used. The SAS has an average calibration-error residual of -27 dB. At this level, our experience indicates that a point-source interferer cannot be tolerated within less than one-eighth of a beamwidth from the desired source.

To simulate the effect of diffuse main-beam multipath interference on direction-finding a source, we conducted an experiment with two horn antennas elevated above the earth. The first antenna was angled downward such that its radiation pattern illuminated the earth, but did not directly radiate toward the receive array. The second horn provided a direct-path signal to simulate the source of interest. The signal fed to the downward-pointing antenna had 30-dB higher gain than that fed to the direct-path antenna, creating a 20-dB interference-to-signal ratio at the SAS. The SAS was positioned at varying distances from the transmitting antenna complex to give a variety of desired source-interference separations.

To examine the effects of spatial antenna segmentation, we initially connected eight receivers to the eight copolarized outer-array subapertures on the SAS. Because of antenna-pattern limitations, the maximum angular separation between the hot spot of

the multipath interference and the desired source was limited to less than one full-array beamwidth. With the separation between the multipath interference and the desired source solely in the vertical dimension, the important topology variable became the number of different vertical subapertures (number of distinct phase centers in the vertical direction) in use.

We analyzed the measured data by using different subsets of the available eight channels to simulate arrays with three, four, and five distinct vertical subapertures, as shown in Figure 5. Figure 6 shows the results of applying a rooting variant of the maxi-

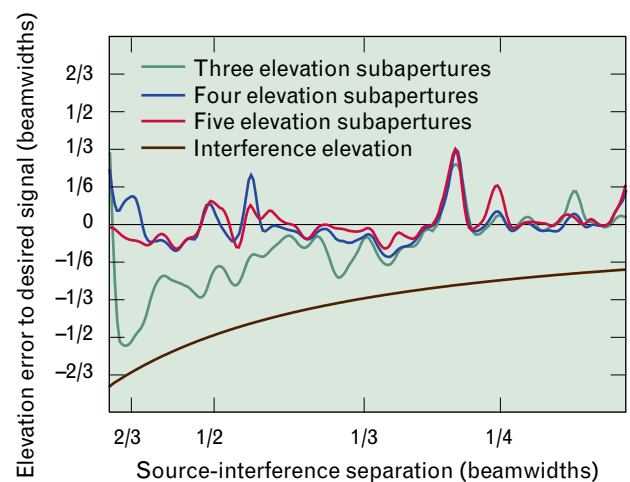


FIGURE 6. Performance of three, four, and five vertical (elevation) subapertures in distinguishing desired signal from diffuse interference. A four- and five-subaperture array performs well but the three-subaperture array fails to find the desired signal.

mum-likelihood method (MLM) algorithm [2] to the three different SAS array configurations. The results show that the estimates closest to the desired source of the three-subaperture array tend to track the interference signal rather than the source, while the four- and five-subaperture arrays more or less track the desired source. This behavior indicates that three subapertures in elevation cannot resolve the desired source from the interference, while four or five subapertures in elevation can resolve and track the desired source.

In addition to resolution, another factor that affects a direction-finding system is the variance of the source-direction parameters produced by the estimating algorithm. Unlike resolution, which can be highly dependent on the algorithm used, estimator variance can be bounded from below by a number of algorithm-independent expressions. One expression, the Cramér-Rao bound, is commonly used to determine limits on estimates generated by arrays [3]. The bound is a function of the subaperture topology. To compute the bound, we calculate the spatial covariance of the interference source. For diffuse multipath sources, the calculation requires knowledge of the reflection coefficients, in this case those of the earth's surface.

By using models such as the Beckmann-Spizzichino model [4], we can calculate the spatial covariance matrix for a diffuse multipath source and a Cramér-Rao bound on the variance of the direction parameters to the desired source. Figure 7 shows that using a six-subaperture array instead of a four-subaperture array decreases the bound on elevation-angle noise for the geometries tested with the SAS by over a factor of two. This improvement can be attributed to the additional vertical phase center in the six-subaperture array. Figure 8 shows that the six-subaperture array has four distinct phase centers in elevation, while the four-subaperture array has only three. This improvement further confirms our desire to have at least four distinct phase centers in the source-interference dimension.

Note that the bound on elevation-angle noise from the four-subaperture array is a minimum for this particular orientation; if the array is rotated such that there are four distinct phase centers in elevation, the bounds on elevation-angle noise actually increase.

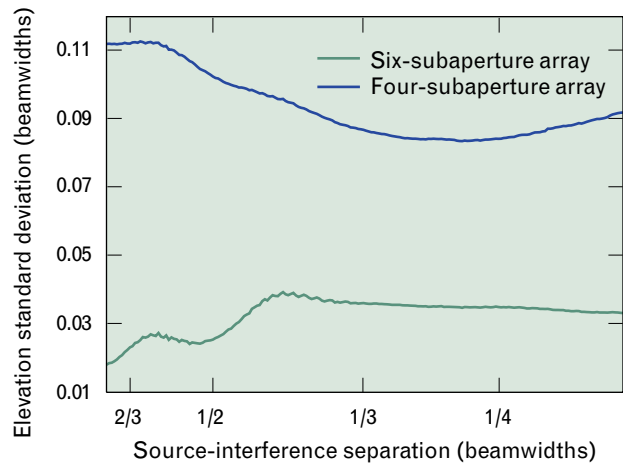


FIGURE 7. Cramér-Rao bounds on elevation-angle noise for four- and six-subaperture arrays. A four-subaperture array does not have enough degrees of freedom to handle the diffuse interference, and thus performs poorly. A six-subaperture array decreases the bound on elevation-angle noise by more than a factor of two for the geometries tested with the SAS.

This increase in the elevation-angle noise bound implies that the number of degrees of freedom is as important as the number of phase centers.

To understand why the elevation-angle noise bounds from the four-subaperture array are so large, we consider the maximum number of point sources for which unambiguous direction estimates can be found, given a planar array of N sensors. A well-known result in the literature indicates that the maximum number of point sources should be $N - 1$ for an arbitrary planar-array geometry [5]. However, when the array is centrosymmetric, this result is no longer

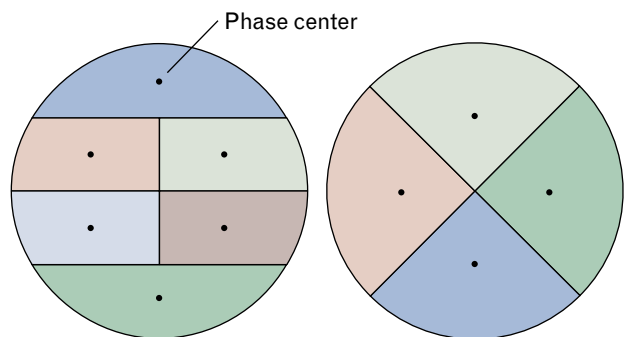


FIGURE 8. Six-subaperture and four-subaperture arrays. The six-subaperture array has four phase centers in elevation, while the four-subaperture array has three.

valid. The appendix entitled “A Maximum Number of Sources Uniquely Localizable with a Centrosymmetric Array” shows that, in this case, only $N - 2$ sources can be unambiguously located. Thus a four-subaperture square array can handle at most two pointlike sources. A diffuse interference source can be thought of as two or more closely spaced point sources. Thus, with respect to degrees of freedom, it seems unlikely that a four-subaperture square array would perform well against a diffuse interference source.

Polarization Diversity

The previous results show that to mitigate diffuse main-beam interference, an array should use a segmentation with more than three subapertures in the line defined by the source-interference pair, and more than four channels. We can further eliminate main-beam interference effects if there are polarization-state differences between the desired signal and the interference, and not all the subapertures of the array have the same polarization response. This approach acknowledges that the difficulty in estimating the direction to a source with main-beam interference is a function of the array-beamspace distance between the desired source array-response vector and the interference array-response vectors. This distance depends on the inner product of the two normalized array-response vectors [6].

For unipolar arrays experiencing main-beam interference, the desired source-interference array-beamspace distance can be mapped monotonically to angular separation between the desired source and interference. With diversely polarized subapertures in the array, such a mapping is not possible because the distance between the desired source array-response vectors and the interference array-response vectors is now a function of not only the angular locations of the desired source and interference, but also their polarization states. Note that just as any polarization-state plane wave can be synthesized by some complex combination of vertical and horizontal plane waves, any array response from a polarization-diverse array can be generated by a complex linear combination of the array response to a purely vertically polarized plane wave \mathbf{a}_v and the array response to a purely hori-

zontally polarized plane wave \mathbf{a}_h . Thus the array-response vector to a desired source from a direction \mathbf{u} with polarization state \mathbf{p} can be written as

$$\mathbf{a}(\mathbf{u}, \mathbf{p}) = [\mathbf{a}_v, \mathbf{a}_h]\mathbf{p},$$

where \mathbf{p} is defined as a two-dimensional complex vector of unit magnitude.

The inner product of the normalized array-response vectors from directions \mathbf{u}_1 and \mathbf{u}_2 with polarization states \mathbf{p}_1 and \mathbf{p}_2 seen by a polarization-diverse array is given by

$$\frac{\mathbf{p}_1^H \begin{bmatrix} \mathbf{a}_v^H(\mathbf{u}_1)\mathbf{a}_v(\mathbf{u}_2) & \mathbf{a}_h^H(\mathbf{u}_1)\mathbf{a}_v(\mathbf{u}_2) \\ \mathbf{a}_v^H(\mathbf{u}_1)\mathbf{a}_h(\mathbf{u}_2) & \mathbf{a}_h^H(\mathbf{u}_1)\mathbf{a}_h(\mathbf{u}_2) \end{bmatrix} \mathbf{p}_2}{\|[\mathbf{a}_v(\mathbf{u}_1), \mathbf{a}_h(\mathbf{u}_1)]\mathbf{p}_1\| \|[\mathbf{a}_v(\mathbf{u}_2), \mathbf{a}_h(\mathbf{u}_2)]\mathbf{p}_2\|}.$$

This equation shows that even if the directions \mathbf{u}_1 and \mathbf{u}_2 are identical, the polarization states \mathbf{p}_1 and \mathbf{p}_2 can have values such that the inner product of the two-array-response vectors can range from zero to one. Thus it may be much easier to estimate the direction to a source with main-beam interference if the receiving array has diversely polarized subapertures, rather than all subapertures of the same polarization. This arrangement, however, comes with a computational cost. Because the array is now sensitive to polarization, the number of parameters that we must estimate to determine the desired source direction includes the polarization state of the source. Consequently, the fast estimation algorithms require an additional degree of freedom, as we discuss later. Thus, instead of needing a four-channel array to estimate the direction parameters to a source in the presence of one pointlike main-beam interferer, a diversely polarized array would require five channels.

The above representation is valid when the polarization states of the plane waves are constant with time. When the polarization state changes during the observation time, the energy that the array sees is not contained in a one-dimensional subspace, as it is for a source of constant polarization, but occupies a two-dimensional subspace spanned by the vertical and horizontal array-response vectors $\mathbf{a}_v(\mathbf{u})$ and $\mathbf{a}_h(\mathbf{u})$. If this condition occurs with the interference energy, it will increase the number of degrees of freedom in the array required to accurately estimate the desired

source direction parameters because the energy from the interference direction acts as if there were two sources. In addition, the distance between the desired source array-response vector and the interference array-response subspace is measured as the closest approach between the interference subspace and the desired source array-response vector. This definition of distance implies that if the polarization state of the interference varies during the observation time, the difficulty in estimating the desired source direction will be determined by the inner product of the desired source array-response vector and the array-response vector from the interference direction with the worst possible polarization state, even if that state is never actually observed.

Data Examples of Polarization Diversity

We conducted an experiment to estimate the desired source directions by using both singly polarized and diversely polarized arrays in the presence of a point-like interferer with a non-fluctuating polarization state. For this experiment, two horns were placed on the ground. The source horn transmitted a continuous tone in a vertically polarized state, while the interference horn radiated a noise waveform, and the horn was tilted so that the polarization was linear at a 45° slant to vertical and had a 20-dB interference-to-signal ratio in the processing band of interest. The singly polarized array was a standard quadrant monopulse configuration. The diversely polarized array consisted of all four vertical monopulse channels plus a horizontally polarized sum and a horizontally polarized azimuth difference beam. The results in Figure 9 show that the addition of the two cross-polarized channels greatly decreases the variance of the source direction estimates.

Estimation Algorithms

The results of our array-topology study indicate that topologies more complicated than simple quadrant arrays, with perhaps some diversely polarized subapertures, are desirable to mitigate main-beam interference. Because of the computational stress that adaptive-array processing entails, efficient algorithms for producing desired source direction estimates are imperative. This section of the article discusses two new

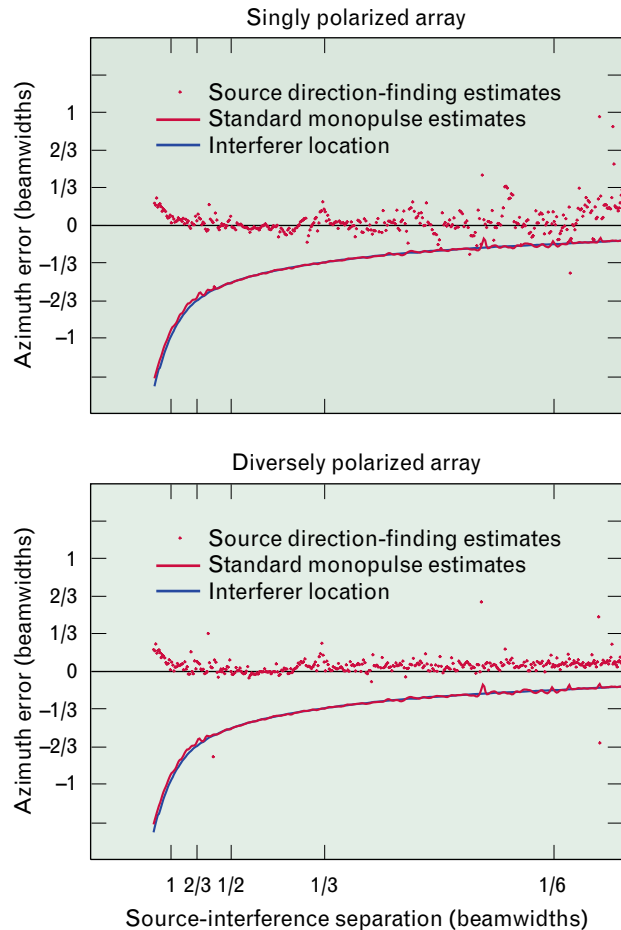


FIGURE 9. Azimuth errors as a function of source-interference separation for a vertically polarized source in the presence of mixed-polarization interference. The improved performance of the diversely polarized array, evidenced by less scattering of data points, can be attributed to its ability to differentiate signal and interference both polarimetrically and spatially.

algorithms designed to efficiently estimate source directions from arbitrary multidimensional arrays. The first algorithm, PRIME, estimates directions for not only the desired source but also for all the interference sources. This algorithm can be used on any type of signal and interference waveform. The second algorithm, GAMMA, provides estimates for only the desired source direction. This algorithm requires that the interference covariance matrix be estimated in the absence of appreciable desired signal energy.

Both algorithms achieve their computational efficiency by posing the angle-estimation problem in such a way that the estimates are generated from the

roots of a data-derived polynomial. To understand the benefits of this technique, we consider a general direction-estimation algorithm. Most modern direction-finding algorithms applied to unipolar arrays can be posed as

$$\mathbf{u}^* = \arg \max_{\mathbf{u}} \frac{\mathbf{a}(\mathbf{u})^H \mathbf{M}_1 \mathbf{a}(\mathbf{u})}{\mathbf{a}(\mathbf{u})^H \mathbf{M}_2 \mathbf{a}(\mathbf{u})}, \quad (2)$$

where \mathbf{u}^* is the source direction estimate, and \mathbf{M}_1 and \mathbf{M}_2 are arbitrary matrices whose exact values depend on the test statistic used.

The difficulty of calculating this test statistic is in finding the maximum over the direction parameters. Attempts at differentiation of the test statistic with respect to the parameters of the direction vector \mathbf{u} typically do not yield simple equations. Thus the extremal values of \mathbf{u} are generally calculated by evaluating the test statistic over a grid of potential values for \mathbf{u} . This approach is often referred to as searching over the array manifold, because the set of array-response vectors $\mathbf{a}(\mathbf{u})$ can be considered a submanifold in complex N -dimensional space (if there are N subapertures) with dimension equal to M , which is the number of parameters in the vector \mathbf{u} . The rough estimates for local maxima are then refined, often by some local gradient iteration algorithm.

When the number of parameters in the direction vector \mathbf{u} becomes larger than one, this manifold search technique can become computationally intensive. Much effort has gone into avoiding this search technique for simple source and interference scenarios with simple array topologies. In the case in which the spatial covariance of the interference is an identity, Equation 2 simplifies to

$$\mathbf{u}^* = \arg \max_{\mathbf{u}} \left| \mathbf{a}(\mathbf{u})^H \mathbf{x} \right|^2.$$

For a quadrant array topology that estimates azimuth and elevation, this problem can be approximately solved by using the monopulse technique. Unfortunately, when main-beam interference is present, this easy approximation does not work.

In the case of a special array topology—a uniformly spaced unipolar line array—another technique has been proposed to avoid the manifold

search. In this case, the array manifold is only a function of a single scalar u and has the form

$$\mathbf{a}(u) = \begin{bmatrix} 1 \\ e^{jku} \\ e^{j2ku} \\ \vdots \\ e^{j(N-1)ku} \end{bmatrix}. \quad (3)$$

The phase center of the array is assumed to be the first subaperture. The constant k is the scaled distance between subapertures, defined as in Equation 1, with d the distance between adjacent subapertures. Reference 7 notes that if a new complex variable, defined as z , is used to replace the term e^{jku} in Equation 2, then $\mathbf{a}(z)$ has the form

$$\mathbf{a}(z) = \begin{bmatrix} 1 \\ z \\ z^2 \\ \vdots \\ z^{N-1} \end{bmatrix}.$$

Reference 7 further notes that when the magnitude of the variable z is unity, then the conjugate of $\mathbf{a}(z)$ is equal to $\mathbf{a}(z^{-1})$. By using these substitutions, we can express Equation 2 as

$$\arg \max_{|z|=1} \frac{\mathbf{a}(z^{-1})^T \mathbf{M}_1 \mathbf{a}(z)}{\mathbf{a}(z^{-1})^T \mathbf{M}_2 \mathbf{a}(z)}.$$

Finally, if the condition $|z| = 1$ is relaxed, then the optimization statistic can be driven to infinity for values of z such that

$$z^{N-1} \mathbf{a}(z^{-1})^T \mathbf{M}_2 \mathbf{a}(z) \equiv g(z) = 0. \quad (4)$$

The z^{N-1} term is added to eliminate negative powers of z , allowing $g(z)$ to be a common polynomial.

This conversion from performing a manifold search required by Equation 2 to solving for a set of homogeneous solutions of a complex polynomial problem was applied to a number of superresolution direction-estimation algorithms, which yielded root-

ing variants of the multiple signal classification (MUSIC) [8] and maximum entropy method (MEM) algorithms [2]. One benefit of the rooting techniques is that they tend to have better resolution properties than previous manifold-search techniques. Reference 2 discusses how the root-MUSIC algorithm resolves two closely spaced sources with a 5-dB-lower signal-to-noise ratio than the spectral (manifold search) MUSIC algorithm. The rooting techniques have been generalized to handle nonuniform linear arrays [1], as well as polarization-diverse linear arrays [9].

By following the logic used to derive a polynomial representation for uniform linear arrays, we can characterize the array manifold for a planar array with subapertures centered on a regular grid in terms of two complex variables. To illustrate this concept, let us assume a rectangular gridding for the subapertures of the array. Consider the subaperture in the upper left corner as the phase-reference element (the phase reference can be arbitrarily chosen anywhere on the array). The array-response vector element $a_{l,p}$ corresponding to the subaperture displaced to the right by l subapertures and down by p subapertures has the form

$$a_{l,p} = e^{(jk_1u_1)l} e^{(jk_2u_2)p} .$$

Here k_1 is the scaled distance between subaperture phase centers in the vertical direction, and k_2 is the scaled distance between subaperture phase centers in the horizontal direction. By making the substitution

$$w = e^{jk_1u_1} \text{ and } z = e^{jk_2u_2} ,$$

we can represent the array-response vector $\mathbf{a}(\mathbf{u})$ as $\mathbf{a}(z, w)$. By using this representation, we can develop a two-variable polynomial equation for a planar array similar to the univariate polynomial in Equation 4. Using this representation does not give unique solutions for either z or w , however, because we have only one equation with two unknowns.

The PRIME algorithm was developed to solve this problem. It is often possible to generate two independent statistics that have local maxima corresponding to true source directions. The system of equations

$$\begin{aligned} g_1(z, w) &= 0 \\ g_2(z, w) &= 0 \end{aligned}$$

defines a finite set of (z, w) pairs that satisfy both polynomials. Some of these solutions correspond to true source locations. Take, for example, the PRIME version of the MUSIC algorithm. As noted in Reference 8, the estimation test statistic in this case is

$$\mathbf{u}^* = \arg \max_{\mathbf{u}} \frac{1}{\mathbf{a}(\mathbf{u})^H \hat{\mathbf{E}}_n \hat{\mathbf{E}}_n^H \mathbf{a}(\mathbf{u})} . \quad (5)$$

Here $\hat{\mathbf{E}}_n$ are estimates of the eigenvectors of the sample covariance matrix (which is $\sum_i \mathbf{x}_i \mathbf{x}_i^H$ by definition) that are orthogonal to all the source array-response vectors, including interference. If the rank of the matrix $\hat{\mathbf{E}}_n$, defined as q , is greater than or equal to two, then we can construct two distinct subsets of the eigenvectors in $\hat{\mathbf{E}}_n$, defined as $\hat{\mathbf{E}}_{n1}$ and $\hat{\mathbf{E}}_{n2}$, where

$$\begin{aligned} \text{rank}\{\hat{\mathbf{E}}_{n1}\} &< q, \text{rank}\{\hat{\mathbf{E}}_{n2}\} < q; \\ \hat{\mathbf{E}}_{n1} &\neq \hat{\mathbf{E}}_{n2} ; \text{and} \\ \hat{\mathbf{E}}_{n1} \cup \hat{\mathbf{E}}_{n2} &= \hat{\mathbf{E}}_n . \end{aligned}$$

By using these two new matrices, we define the polynomials $g_1(z, w)$ and $g_2(z, w)$ as

$$\begin{aligned} g_1(z, w) &= \\ & z^{N_1-1} w^{N_2-1} \mathbf{a}(z^{-1}, w^{-1})^T \hat{\mathbf{E}}_{n1} \hat{\mathbf{E}}_{n1}^H \mathbf{a}(z, w) \\ g_2(z, w) &= \\ & z^{N_1-1} w^{N_2-1} \mathbf{a}(z^{-1}, w^{-1})^T \hat{\mathbf{E}}_{n2} \hat{\mathbf{E}}_{n2}^H \mathbf{a}(z, w) . \end{aligned}$$

The scalars N_1 and N_2 are the number of phase centers in the elevation and azimuth planes of the array, respectively. Note that in the absence of estimation error and array-calibration errors, the expressions

$$\begin{aligned} \mathbf{a}(z^{-1}, w^{-1})^T \hat{\mathbf{E}}_{n1} \hat{\mathbf{E}}_{n1}^H \mathbf{a}(z, w) \\ \mathbf{a}(z^{-1}, w^{-1})^T \hat{\mathbf{E}}_{n2} \hat{\mathbf{E}}_{n2}^H \mathbf{a}(z, w) \end{aligned}$$

are zero for (z, w) pairs corresponding to true source directions, just as the original term

$$\mathbf{a}(z^{-1}, w^{-1})^T \hat{\mathbf{E}}_n \hat{\mathbf{E}}_n^H \mathbf{a}(z, w)$$

is zero. Thus some joint solutions to these two equations correspond to directions having array-response vectors orthogonal to $\hat{\mathbf{E}}_n$, maximizing Equation 5.

There are other methods for forming multiple in-

dependent polynomials. One method is to form independent statistics on two nonsimilar subarrays of the entire array aperture. This method allows us to incorporate a larger number of subapertures into the direction-estimation problem than the number of available receivers. Figure 10 provides an example of two dissimilar subarrays from a segmented array. A third method is to differentiate the original polynomial $g(z, w)$ with respect to both z and w . This approach generates two new independent polynomials that retain the homogeneous solution properties of the original statistic.

Polynomial Root Intersections

The heart of the PRIME algorithm is the formation of polynomial root intersections. For the cases treated here, root intersection means finding the common zeros of two polynomials in two unknowns. Several procedures are relevant. First, numerical techniques can be used if good initial guesses are available. A more sophisticated global approach utilizes root tracking and homotopy (e.g., linear interpolation) of the polynomial coefficients from a canonical, decoupled set of equations to the equations of interest [10]. This approach is most appropriate when the polynomials have high degree. For lower-degree polynomials, a simpler procedure known as elimination theory provides all intersection points. We now present a mathematical explanation of elimination theory.

Consider two polynomials $f(x)$ and $g(x)$ of a single

variable with, for example, complex coefficients:

$$f(x) = a_n x^n + \dots + a_1 x + a_0$$

$$g(x) = b_m x^m + \dots + b_1 x + b_0.$$

Let $\{\gamma_i\}$ and $\{\delta_i\}$ denote the roots of f and g , respectively. The resultant R of the two polynomials f and g is given by Reference 11:

$$R(f, g) \equiv a_n^m b_m^n \prod_{ij} (\gamma_i - \delta_j).$$

$R(f, g)$ can be shown to be a polynomial in the coefficients $\{a_i\}$ and $\{b_j\}$ of the polynomials f and g that vanishes if and only if $f(x)$ and $g(x)$ have a common root, provided at least one of a_n and b_m is nonzero. There are several different but equivalent expressions for the resultant. One of the simplest, from Sylvester [12], expresses $R(f, g)$ as the determinant of the $(m+n) \times (m+n)$ matrix

$$\begin{bmatrix} a_n & a_{n-1} & \dots & a_0 & 0 & \dots & 0 \\ 0 & a_n & a_{n-1} & \dots & a_0 & \dots & 0 \\ \vdots & \vdots & \vdots & \vdots & \vdots & \vdots & \vdots \\ 0 & \dots & 0 & a_n & \dots & a_1 & a_0 \\ b_m & b_{m-1} & \dots & b_0 & 0 & \dots & 0 \\ 0 & b_m & b_{m-1} & \dots & b_0 & \dots & 0 \\ \vdots & \vdots & \vdots & \vdots & \vdots & \vdots & \vdots \\ 0 & \dots & 0 & b_m & \dots & b_1 & b_0 \end{bmatrix}.$$

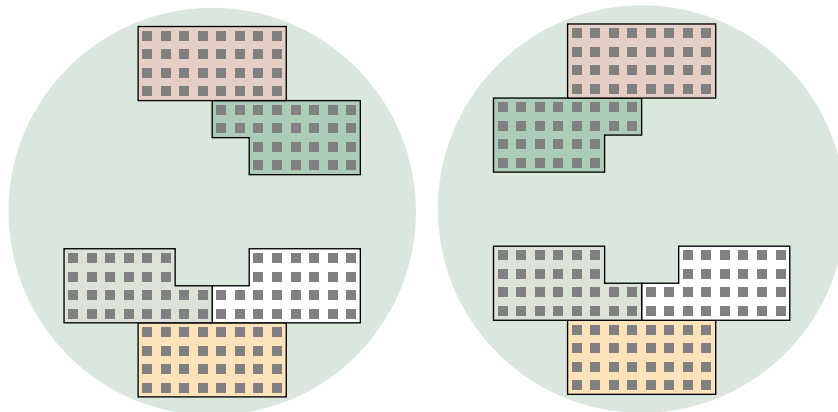


FIGURE 10. Two dissimilar five-subaperture subarrays from a six-subaperture array. These configurations allow us to incorporate a larger number of subapertures into the direction-estimation problem than the number of available receivers.

PRIME must find the root intersections of two-variable polynomials $g_1(z, w)$ and $g_2(z, w)$. If we view g_1 and g_2 as polynomials in w with coefficients that are polynomials in z , the resultant, denoted $R_w(z)$, is a polynomial in z whose roots are the z -coordinates of the common solutions of $g_i(z, w) = 0$. Similarly, the resultant $R_z(w)$ is a polynomial in w expressing the w -coordinates. For small degrees, we can determine the roots of the resultants R_z and R_w and pair the resulting z - w coordinates in all possible ways to form a list of candidate intersections that we can substitute in the original equations. Alternatively, we can calculate the homogeneous solutions for R_z and substitute them in the original polynomials g_1 or g_2 .

Not all common roots of $g_i(z, w)$ correspond to physical angles. We can select physically relevant roots by evaluating a direction-finding statistic such as spectral MUSIC for each common root or by utilizing prior information about signal angles of arrival. If $R_w(z)$, or $R_z(w)$, vanishes identically, the polynomials $g_i(z, w) = 0$ have a common nontrivial factor (assuming, for example, that the coefficient of the highest w -order term of $g_1(z, w)$ or $g_2(z, w)$ is a nonzero polynomial in z). In this case, the solution sets intersect along the curve defined by the common factor. This case is not typically encountered in applications. However, sometimes the $g_i(z, w)$ have a common data-independent factor (typically of the form $z^L w^N$) that can be eliminated from both polynomials.

The number of intersection points of the root loci $g_i(z, w)$ depends on the polynomial degrees, the array geometry, and any symmetries inherent in the polynomial coefficients, which in turn depend on the polynomial selection procedure. Let d_i denote the degrees of g_i . A bound on the number of intersection points can be based on Bezout's theorem, which states that after accounting for and including roots at infinity, the number of common solutions of the homogenized polynomials, for $i = 1$ and 2 , is $d_1 \times d_2$. The polynomials typically used for direction finding share degenerate roots at infinity (i.e., common solutions involving only the highest-order terms of each polynomial). By accounting for the multiplicity of these roots at infinity, we can formulate a bound on the number of roots (including multiplicity) in the finite z - w plane. Alternatively, we can apply a result of A.G.

Kouchnirenko [13] to count the number of common roots of polynomials. For example, an $m \times n$ array generically provides $2(m - 1)(n - 1)$ roots, with both z and w nonzero.

While this discussion has concentrated on the case of a unipolar planar array, note that elimination theory can be extended to polynomials of more than two variables. Hence, in the case of polarization-diverse planar arrays, where the array-response vectors can be described as functions of three complex scalars (z , w , and the polarization ratio ρ), the PRIME method may still be applied. In this case, three poly-

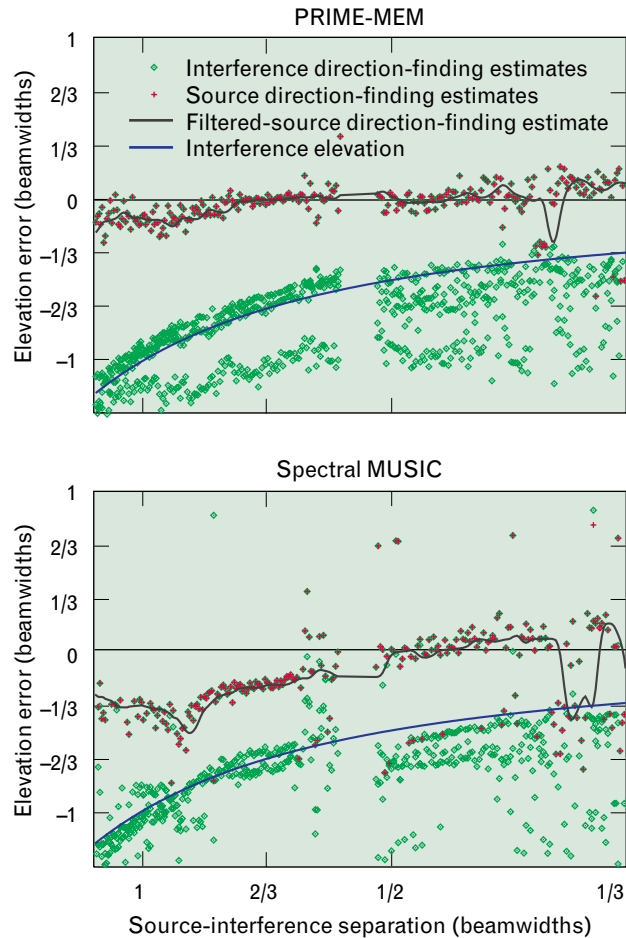


FIGURE 11. The polynomial root intersection for multidimensional estimation (PRIME) maximum entropy method (MEM), top, versus spectral multiple signal classification (MUSIC) direction estimation with diffuse interference, bottom. The PRIME-MEM source-location estimates have fewer points captured by the interference when the signal-interference separation is small, and the source-location estimates are not as biased when the separation is large.

nomials must be generated instead of two, but otherwise the technique is similar to that of the unipolar planar-array case. In fact, the PRIME technique can be extended to non-planar arrays, where the phase centers of the subapertures now lie on a three-dimensional lattice of points, by adding a third variable corresponding to the displacement in depth of the sensors. The existence of these generalizations makes the PRIME technique powerful.

We have analyzed the asymptotic (in data snapshots) accuracy of the PRIME versions of algorithms such as MUSIC (see the appendix entitled “Asymptotic Mean-Squared Error for PRIME Direction Estimates”), and we can prove that under mild constraints on array topology, the accuracy of the PRIME versions of the algorithms can equal that of the spectral versions.

Data Examples of Polynomial Root Intersections

Figure 11 shows an example of the performance of a PRIME-based algorithm compared with a two-dimensional spectral-MUSIC algorithm, in which both algorithms attempt to track a source in the presence of diffuse main-beam interference. In this case, the received interference-to-signal ratio was roughly 20 dB, and as the range to the desired source decreased, the angular separation between the source and the interference increased. We took the data with the SAS antenna by using six subapertures of the vertically polarized outer-array configuration. These six subapertures are shown in the middle configuration in Figure 5. Notice that the number of points where the desired source is not resolved is much lower for the PRIME algorithm than for the spectral-MUSIC algorithm. Also notice that the spectral-MUSIC algorithm begins to exhibit a large amount of bias as the angular extent of the interference increases (as the angular separation between the desired source and the interference increases), while the PRIME algorithm does not suffer from this problem.

Waveform Exploitation

Sometimes we can estimate the spatial distribution of the interference without the presence of the desired source signal. One example of this scenario is a time-gated signal (satisfied by most range-resolving radar

waveforms), in which the interference is a non-gated broadband noise source. The received signals in between source pulse returns consist only of interference and noise signals. As mentioned in Reference 6, waveform knowledge can be a powerful tool in resolving source signals from interference. In the case in which the interference has a high interference-to-noise ratio, the maximum-likelihood-optimal estimate for the source direction [14] can again be expressed as in Equation 1. The estimate is defined as

$$\mathbf{u}^* = \arg \max_{\mathbf{u}} \frac{\mathbf{a}(\mathbf{u})^H \hat{\mathbf{R}}_i^{-1} \hat{\mathbf{R}}_x \hat{\mathbf{R}}_i^{-1} \mathbf{a}(\mathbf{u})}{\mathbf{a}(\mathbf{u})^H \hat{\mathbf{R}}_i^{-1} \mathbf{a}(\mathbf{u})}, \quad (6)$$

where $\hat{\mathbf{R}}_i$ is the sampled covariance matrix of the interference plus noise, and $\hat{\mathbf{R}}_x$ is the sampled covariance matrix of the desired source plus the interference. In developing the PRIME technique, we noted that by driving the denominator of the optimization expression to zero, we maximized the overall expression. In this case, unfortunately, we cannot ignore the numerator of the test statistic, since all of the desired source information is contained in the numerator.

An alternate option is to rewrite Equation 6 in the form

$$\arg \max_{\mathbf{u}} \frac{\mathbf{a}(\mathbf{u})^H \hat{\mathbf{R}}_i^{-1/2} \hat{\mathbf{R}}_x^{-1/2} \hat{\mathbf{R}}_i^{-1/2} \hat{\mathbf{R}}_x \hat{\mathbf{R}}_i^{-1/2} \hat{\mathbf{R}}_i^{-1/2} \mathbf{a}(\mathbf{u})}{\mathbf{a}(\mathbf{u})^H \hat{\mathbf{R}}_i^{-1/2} \hat{\mathbf{R}}_i^{-1/2} \mathbf{a}(\mathbf{u})}. \quad (7)$$

The expression can now be viewed as taking the induced inner product of a normalized whitened array-response vector $\hat{\mathbf{R}}_i^{-1/2} \mathbf{a}(\mathbf{u}) \equiv \mathbf{a}_w(\mathbf{u})$ through the whitened source-plus-interference covariance matrix $\hat{\mathbf{R}}_i^{-1/2} \hat{\mathbf{R}}_x \hat{\mathbf{R}}_i^{-1/2} \equiv \hat{\mathbf{R}}_w$. These terms are referred to as whitened because the covariance of the interference component in the source-plus-interference covariance matrix is an identity, or spatially white. Thus in expectation, the test statistic (Equation 7) can be written as

$$\begin{aligned} \arg \max_{\mathbf{u}} & \frac{\mathbf{a}_w(\mathbf{u})^H \mathbf{a}_w(\mathbf{u})}{\mathbf{a}_w(\mathbf{u})^H \mathbf{a}_w(\mathbf{u})} + \sigma_s^2 \frac{\mathbf{a}_w(\mathbf{u})^H \mathbf{e}_w \mathbf{e}_w^H \mathbf{a}_w(\mathbf{u})}{\mathbf{a}_w(\mathbf{u})^H \mathbf{a}_w(\mathbf{u})} \\ & = \arg \max_{\mathbf{u}} \frac{\mathbf{a}_w(\mathbf{u})^H \mathbf{e}_w \mathbf{e}_w^H \mathbf{a}_w(\mathbf{u})}{\mathbf{a}_w(\mathbf{u})^H \mathbf{a}_w(\mathbf{u})}. \end{aligned} \quad (8)$$

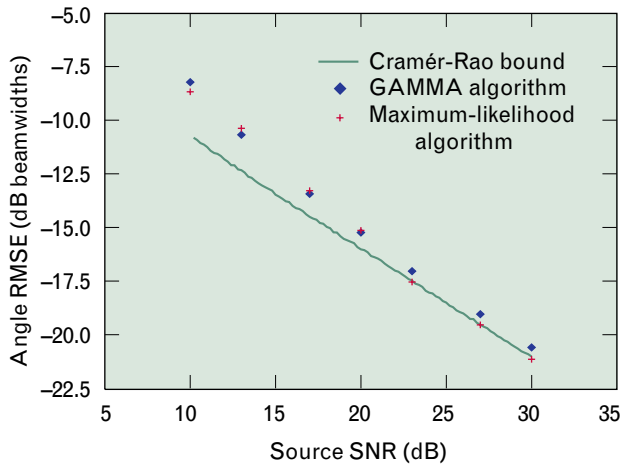


FIGURE 12. Computer simulation of GAMMA-estimate root-mean-squared error (RMSE) compared to the RMSE of the maximum-likelihood-optimal estimation algorithm. The GAMMA estimate tracks the performance of the optimal estimator over a wide range of source signal-to-noise ratio (SNR). The Cramér-Rao bound is included for reference.

Here σ_s^2 is the signal-to-noise ratio of the desired source, and \mathbf{e}_w is the whitened array-response vector of the desired source. An estimate of the vector \mathbf{e}_w can be derived from the data by taking the principal eigenvector $\hat{\mathbf{e}}_w$ of the matrix $\hat{\mathbf{R}}_w$. Using this derivation, we can approximate Equation 6 as

$$\begin{aligned} \arg \max_{\mathbf{u}} \frac{\mathbf{a}_w(\mathbf{u})^H \hat{\mathbf{e}}_w \hat{\mathbf{e}}_w^H \mathbf{a}_w(\mathbf{u})}{\mathbf{a}_w(\mathbf{u})^H \mathbf{a}_w(\mathbf{u})} \\ = \arg \max_{\mathbf{u}, \alpha} \|\alpha \mathbf{a}_w(\mathbf{u}) - \hat{\mathbf{e}}_w\|^2. \end{aligned} \quad (9)$$

This last form of the test statistic has eliminated all functions of the direction parameters \mathbf{u} from the denominator by introducing a nuisance scale factor α . This expression defines a test that finds the best whitened array-response vector that minimizes the error vector between the appropriately scaled whitened array-response vector and the estimated whitened source array-response vector.

The solution to the test statistic in Equation 9 is a generalized monopulse solution. The monopulse technique can be thought of as finding the \mathbf{u} that maximizes Equation 9 when the whitening matrix $\hat{\mathbf{R}}_i^{-1/2}$ is the identity matrix, and thus $\mathbf{a}_w(\mathbf{u}) = \mathbf{a}(\mathbf{u})$ and, for a single pulse, $\hat{\mathbf{e}}_w = \mathbf{x}$. The monopulse tech-

nique projects the error vector $\alpha \mathbf{a}_w(\mathbf{u}) - \hat{\mathbf{e}}_w$ onto the subspace spanned by the steering vector of the assumed source direction, and the partial derivative of that vector with respect to the desired source parameters u_i . This technique creates an $(M + 1)$ -dimensional subspace, where M is the number of source parameters desired. The projected error is then driven to zero by choosing the correct α and \mathbf{u} . In the case of no interference and spatially white noise, the equations giving the parameters \mathbf{u} decouple into the familiar monopulse ratio expressions for either linear or planar arrays.

When the array has subapertures with phase centers that lie on a grid, then just as in the PRIME algorithm, the array-response vectors can be characterized as polynomial functions of complex parameters. Again, for a planar array this characterization requires two parameters. If the monopulse projection is done on the error vector when interference is present in the environment, driving the projected error vector to zero norm will generate $M + 1$ coupled nonlinear polynomial equations (here, $M + 1$ equals 3) in the variables α , z , and w . In this case the projection matrix is spanned by the whitened assumed array-response vector of the source, as well as the whitened derivative vectors of the assumed source array-response vector with respect to the desired parameters to be estimated. This projection matrix can be shown

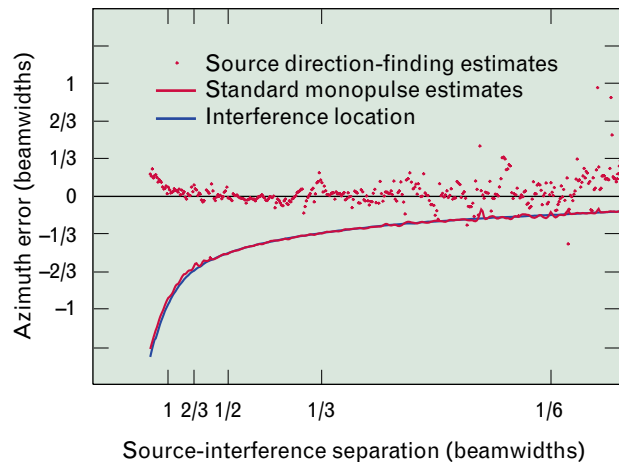


FIGURE 13. GAMMA direction azimuth errors for pointlike main-beam interference scenario. The desired signal direction can be estimated with strong interference less than one-quarter of a beamwidth away.

to be locally optimal for estimating the desired source parameters.

We can solve the equations directly for α because they are linear in α , leaving two polynomial equations in z and w . Just as in the PRIME algorithm, we can solve these equations by using resultant methods. This new algorithm, GAMMA, has shown statistical efficiencies virtually equaling that of the true maximum-likelihood estimator (Figure 12), while requiring no computationally expensive manifold search.

We note that just as the PRIME algorithm can be extended to polarization-diverse arrays and three dimensional arrays, so can the GAMMA algorithm. In fact, we generated the polarization-diverse array results in Figure 9 by using the polarization-diverse version of the GAMMA algorithm.

Data Example of Waveform Exploitation

We applied the GAMMA algorithm to real array data. In this test, the desired source was a transmitting horn placed on the ground, producing a continuous-wave tone. The interference was another ground-based horn, placed some distance from the first, transmitting a noise waveform. We set the power of the interference so that the signal-to-interference ratio was -20 dB in the narrow frequency cell used to process the desired tone. Then we derived the estimate of the spatial covariance of the interference by using frequency cells away from the desired tone cell. Figure 13 shows how the desired signal track develops while the interference is still well within the main beam of the receive antenna.

Conclusion

In this article, we have put forth design concepts for planar-array direction-finding systems that are intended to be robust in the face of main-beam interference. We presented results of an antenna-subaperture configuration study that showed the desirability of more complex subaperture configurations than the standard monopulse configuration, specifically to counter diffuse main-beam interference. Results from both theoretical bounds and tests confirm the advantage of using four subapertures in elevation with five or more receiver channels. In addition, we showed that further advantage may be gained by mixing the

polarization of the array subapertures. This gain comes at a price, however, since processing data from a diversely polarized array when it is faced with the same interference scenario requires more channels (and therefore more receivers) than unipolar arrays.

The second section of the article presented two new algorithms for the efficient estimation of source-direction parameters in the presence of main-beam interference. The new algorithms, polynomial root intersection for multidimensional estimation (PRIME) and generalized adaptive multidimensional monopulse algorithm (GAMMA), extend the concept of polynomial rooting algorithms to the realm of planar arrays. The PRIME family of algorithms allows the higher resolution and lower computational cost of a rooting algorithm when attempting to estimate the directions of multiple main-beam sources. The PRIME algorithm's advantages are demonstrated in the case of a source plus diffuse main-beam interference, in which a PRIME algorithm outperforms a conventional two-dimensional spectral superresolution algorithm. In addition, we showed that the asymptotic mean squared error for techniques such as PRIME-MUSIC can be, under certain benign conditions, equal to that of the spectral algorithms they replace.

The GAMMA technique is a computationally efficient method for calculating a nearly maximum-likelihood-optimal solution to the direction-estimation problem in the case of estimatable interference spatial distribution. We showed that GAMMA is the logical extension of monopulse-like algorithms to cases in which the interference background is no longer uncorrelated sensor to sensor. Finally, we presented experimental data that showed the ability to estimate source-direction parameters in the presence of pointlike main-beam interference.

REFERENCES

1. L.L. Horowitz, "Airborne Signal Intercept for Wide-Area Battlefield Surveillance," *Linc. Lab. J.*, in this issue.
2. A.J. Barabell, J. Capon, D.F. DeLong, J.R. Johnson, and K.D. Senne, "Performance Comparison of Superresolution Array Processing Algorithms," *Project Report TST-72*, Lincoln Laboratory (9 May 1984, rev. 15 June 1998).
3. H.L. Van Trees, *Detection, Estimation, and Modulation Theory, Pt. I* (Wiley, New York, 1968).
4. P. Beckman and A. Spizzichino, *The Scattering of Electromagnetic Waves from Rough Surfaces* (Pergamon Press, New York, 1963).
5. M. Wax and I. Ziskind, "On Unique Localization of Multiple Sources by Passive Sensor Arrays," *IEEE Trans. Acoust. Speech Signal Process.* 37 (7), 1989, pp. 996–1000.
6. K.W. Forsythe, "Utilizing Waveform Features for Adaptive Beamforming and Direction Finding with Narrowband Signals," *Linc. Lab. J.*, in this issue.
7. J.E. Evans, J.R. Johnson, and D.F. Sun, "Applications of Advanced Signal Processing Techniques to Angle of Arrival Estimation in ATC Navigation and Surveillance Systems," *Technical Report 582*, Lincoln Laboratory (23 June 1982), DTIC #ADA-118306.
8. R. Schmidt, "Multiple Emitter Location and Signal Parameter Estimation," *Proc. RADC Spectrum Estimation Workshop, Rome, N.Y., 3–5 Oct. 1979*, pp. 243–258.
9. A.J. Weiss and B. Friedlander, "Direction Finding for Diversely Polarized Signals Using Polynomial Rooting," *IEEE Trans. Signal Process.* 41 (5), 1993, pp. 1893–1905.
10. T.-Y. Li, T. Sauer, and J.A. York, "The Cheater's Homotopy: An Efficient Procedure for Solving Systems of Polynomial Equations," *SIAM J. Numer. Anal.* 26 (5), 1989, pp. 1241–1251.
11. B.L. van der Waerden, *Modern Algebra, Vols. 1 and 2* (Ungar, New York, 1953).
12. *Discriminants, Resultants, and Multidimensional Determinants*, I.M. Gelfand, M.M. Kapranov, and A.V. Zelevinsky, (Birkhauser, Boston, 1994).
13. A.G. Kouchnirenko, "Polyèdres de Newton et Nombres de Milnor," *Invent. Math.* 32, 1976, pp. 1–31.
14. E.J. Kelley and K.W. Forsythe, "Adaptive Detection and Parameter Estimation for Multidimensional Signal Models," *Technical Report 848*, Lincoln Laboratory (19 Apr. 1989), DTIC #ADA-208971.
15. G.F. Hatke, "Conditions for Unambiguous Source Location Using Polarization Diverse Arrays," *27th Asilomar Conf. on Signals, Systems & Computers 2, Pacific Grove, Calif., 1–3 Nov. 1993*, pp. 1365–1369.
16. C.P. Mathews and M.D. Zoltowski, "Eigenstructure Techniques for 2-D Angle Estimation with Uniform Linear Arrays," *IEEE Trans. Signal Process.* 42 (9), 1994, pp. 2395–2407.

APPENDIX A: MAXIMUM NUMBER OF SOURCES UNIQUELY LOCALIZABLE WITH A CENTROSYMMETRIC ARRAY

ASSUME A CENTROSYMMETRIC array of N elements. There exists a beamformer that transforms the array-response vector $\mathbf{a}(\mathbf{u})$ for any value of \mathbf{u} into a beamspace array-response vector $\mathbf{a}_r(\mathbf{u})$, where all components of $\mathbf{a}_r(\mathbf{u})$ are strictly real and independent of \mathbf{u} . Consider the spatial covariance matrix \mathbf{R}_{xx} of the beamformed outputs from the array due to K -plane wave signals plus spatially white noise. This matrix will have the form

$$\mathbf{R}_{xx} = \mathbf{A}_r(\mathbf{U})\mathbf{R}_{ss}\mathbf{A}_r(\mathbf{U})^H + \sigma_n^2\mathbf{I}, \quad (1)$$

where σ_n^2 is the noise power, \mathbf{R}_{ss} is the $K \times K$ source covariance matrix, and

$$\mathbf{A}_r(\mathbf{U}) \equiv [\mathbf{a}_r(\mathbf{u}_1), \dots, \mathbf{a}_r(\mathbf{u}_K)]$$

is the collection of K array-response vectors for the K sources. The matrix $\mathbf{A}_r(\mathbf{U})$ is real, since $\mathbf{a}_r(\mathbf{u}_i)$ is real for all i . Now consider the case in which the source covariance matrix is real (an example of this is if the sources are independent). In this case, the matrix \mathbf{R}_{xx} is real and symmetric.

Because the sample covariance matrix is a sufficient statistic for estimating the direction parameters \mathbf{U} for Gaussian signals [6], it is sufficient to study the information in the spatial covariance matrix in order to determine whether K Gaussian sources can be uniquely localized. One method of determining a necessary condition on the number of signals K is to simply count the number of real parameters that must be estimated to determine \mathbf{U} , and compare that to the number of real scalars available in estimating the covariance matrix \mathbf{R}_{xx} . Reference 15 shows that if there is any chance of ambiguity in estimating any of the parameters (source directions or source correlations), then there must be ambiguity in estimating the source directions. In the case of a real \mathbf{R}_{ss} , the number of parameters available in \mathbf{R}_{xx} is $(N^2 + N)/2$. The number of real parameters involved in the model

of the spatial covariance matrix as stated in Equation 1 is $2K + (K^2 + K)/2 + 1$, with $2K$ parameters corresponding to the directions \mathbf{U} , $(K^2 + K)/2$ corresponding to the elements of the unknown (but real symmetric) source covariance matrix, and one parameter for the noise power.

In order for the parameters to be estimated uniquely, their number must be less than or equal to the number of scalars uniquely determined in estimating \mathbf{R}_{xx} from the data, which we have determined to be $(N^2 + N)/2$. Thus a necessary condition is

$$\frac{N^2 + N}{2} \geq 2K + \frac{K^2 + K}{2} + 1. \quad (2)$$

Now consider $K = N - 1$. Then Equation 2 requires that $2 \geq 2N$, which will not hold true for the minimum number of antennas needed to estimate the direction of one signal. Now consider $K = N - 2$. In this case, Equation 2 holds for all values of N . Hence a necessary condition for unique localization is that the number of sources must be less than or equal to $N - 2$.

APPENDIX B: ASYMPTOTIC MEAN-SQUARED ERROR FOR PRIME DIRECTION ESTIMATES

LET $\mathbf{a}(\alpha, \beta)$ denote the array response of a planar array as a function of the angles $\mathbf{v} = (\alpha, \beta)$. For applications, we can think of $\alpha = 2\pi u_x d_x / \lambda$ and $\beta = 2\pi u_y d_y / \lambda$, where (u_x, u_y, u_z) are the direction cosines for a signal arriving with wavelength λ at a planar x - y array whose elements lie on a rectangular grid with x -spacing d_x and y -spacing d_y . We can write the spectral-MUSIC function as

$$\frac{\mathbf{a}^H(\mathbf{v})\mathbf{a}(\mathbf{v})}{\mathbf{a}^H(\mathbf{v})\hat{\mathbf{P}}_N\mathbf{a}(\mathbf{v})},$$

where $\hat{\mathbf{P}}_N$ denotes the noise-space projector based on the sample covariance matrix. The \mathbf{v} -coordinates of local maxima provide angle estimates. We let $\mathbf{R} = [\mathbf{E}_S\mathbf{E}_N]\Lambda[\mathbf{E}_S\mathbf{E}_N]^H$ express the eigenanalyzed true covariance matrix with ordered eigenvalues in the diagonal matrix Λ and associated normalized eigenvectors in the columns of the signal-subspace matrix \mathbf{E}_S and the noise-subspace matrix \mathbf{E}_N .

We approximate the noise-subspace projector asymptotically in the number of samples L as

$$\hat{\mathbf{P}}_N \approx \mathbf{P}_N + \mathbf{E}_S\mathbf{B}_N^H + \mathbf{E}_N\mathbf{B}^H\mathbf{E}_S^H,$$

where \mathbf{B} is an $M \times (M - S)$ array with independent, mean-zero, complex circular Gaussian entries of covariance

$$E\left[|B_{jk}|^2\right] = L^{-1} \frac{\lambda_j \lambda}{(\lambda_j - \lambda)^2}$$

for $1 \leq j \leq S$ and $1 \leq k \leq M - S$, and where

$$\lambda_1 \geq \dots \geq \lambda_S > \lambda_{S+1} = \dots = \lambda_M \equiv \lambda$$

are the ordered eigenvalues of the spatial covariance and S is the signal-subspace dimension. Let $\mathbf{v}_\Delta \equiv \mathbf{v} - \mathbf{v}_0$ express the estimation error, where \mathbf{v}_0 is the true direction of arrival. We then define the matrix

$$\mathbf{D} \equiv L^{-1} \text{diag}\left(\frac{\lambda_1 \lambda}{(\lambda_1 - \lambda)^2}, \dots, \frac{\lambda_S \lambda}{(\lambda_S - \lambda)^2}\right).$$

Let \mathbf{a}_α and \mathbf{a}_β be α and β partial derivatives of $\mathbf{a}(\alpha, \beta)$. Also let $\Re(\cdot)$ denote the real part of its argument. We use the asymptotic approximation of the noise-space projector given above and the notation just introduced to write the asymptotic variance of the estimation error as [16]

$$E\left[\mathbf{v}_\Delta \mathbf{v}_\Delta^T\right] \approx \frac{1}{2} (\mathbf{a}^H \mathbf{E}_S \mathbf{D} \mathbf{E}_S^H \mathbf{a}) \times \left\{ \Re \begin{pmatrix} \mathbf{a}_\alpha^H P_N \mathbf{a}_\alpha & \mathbf{a}_\alpha^H P_N \mathbf{a}_\beta \\ \mathbf{a}_\beta^H P_N \mathbf{a}_\alpha & \mathbf{a}_\beta^H P_N \mathbf{a}_\beta \end{pmatrix} \right\}^{-1}.$$

Let z equal $e^{i\alpha}$ and w equal to $e^{i\beta}$ be the unit circle elements corresponding to the angles \mathbf{v} equal to (α, β) . Henceforth, z and w are allowed to take values off the unit circle, in which case their phases correspond to angle estimates. The true angles of a signal are denoted \mathbf{v}_0 equal to (α_0, β_0) , and $(z_0, w_0) = (e^{i\alpha_0}, e^{i\beta_0})$.

PRIME utilizes arrays whose elements lie on a planar grid. The elements can be indexed by integer pairs. Let the (j, k) th element have response $\gamma_{jk} z^j w^k$, where

$$-\frac{(N-1)}{2} \leq j, k \leq \frac{(N-1)}{2}.$$

The γ_{jk} are not assumed to have any pattern variations. The array-response vector has apparent size N^2 , for example, when N is even. Some of the γ_{jk} , however, are allowed to vanish. This concession is taken into account by dropping these elements from the array-response vector so that its actual length is denoted M , as above. The array response can then be written

as a vector $\mathbf{a}(z, w)$ with monomial entries satisfying

$$\mathbf{a}(e^{i\alpha}, e^{i\beta}) \equiv e^{iN_z\alpha} e^{iN_w\beta} \mathbf{a}(\alpha, \beta)$$

for appropriately chosen N_z and N_w . To rephrase two-dimensional spectral-MUSIC accuracy results in terms of the monomial vector $\mathbf{a}(z, w)$ and its derivatives, we define

$$\begin{aligned} \mathbf{G} &\equiv \begin{pmatrix} e^{i\alpha_0} & 0 \\ 0 & e^{i\beta_0} \end{pmatrix} \\ \delta &\equiv \mathbf{a}^H(\alpha_0, \beta_0) \mathbf{E}_S \mathbf{D} \mathbf{E}_S^H \mathbf{a}(\alpha_0, \beta_0) \\ &= \mathbf{a}^H(z_0, w_0) \mathbf{E}_S \mathbf{D} \mathbf{E}_S^H \mathbf{a}(z_0, w_0) \\ C_N &\equiv \mathbf{G}^H [\mathbf{a}_z, \mathbf{a}_w]^H P_N [\mathbf{a}_z, \mathbf{a}_w] \mathbf{G}. \end{aligned}$$

Then the asymptotic accuracy of two-dimensional MUSIC can be written as

$$E[\mathbf{v}_\Delta \mathbf{v}_\Delta^T] \approx \frac{\delta}{2} (\Re C_N)^{-1}.$$

This expression can be simplified slightly when the array is centrosymmetric. Centrosymmetry holds when $|\gamma_{jk}| = |\gamma_{-j-k}|$. For example, if the γ_{jk} are all either one or zero, then the elements are paired about a common phase center, with each element of a pair at opposite ends of a diameter through the phase center. Of course there can be an element at the phase center that can be considered paired with itself. For centrosymmetric arrays and signals that are not fully correlated, C_N is real.

One version of PRIME is based on a polynomial built from the denominator of the MUSIC function. We let

$$F(z, w) \equiv z^J w^K \mathbf{a}^T(z^{-1}, w^{-1}) \hat{P}_N \mathbf{a}(z, w),$$

where J and K are chosen to make $F(z, w)$ a polynomial. With infinite samples (i.e., $\hat{P}_N = P_N$), $F(z, w)$ has double roots in z at $z = z_0$ for fixed $w = w_0$. Similarly, $F(z, w)$ has double roots in w for fixed $z = z_0$. Thus the partials F_z and F_w have a common root at (z_0, w_0) . The method of intersecting these partials is called the partial-derivative method. Angle estimates (α, β) are obtained from the angular components of (z, w) . The estimates have the same asymptotic accu-

racy as those of two-dimensional spectral MUSIC as described above.

Another implementation of PRIME is based on choosing noise-subspace probes (a special case of subspace division PRIME-MUSIC). This method provides polynomials of smaller degree than those obtained from partial derivatives. For two M -vectors, \mathbf{q}_i , we define two polynomials

$$g_i(z, w) \equiv \mathbf{q}_i^H \hat{P}_N \mathbf{a}(z, w), \text{ for } i = 1, 2.$$

The common roots provide estimates of (z_0, w_0) . Let $\rho_\delta \equiv (z - z_0, w - w_0)$ represent the estimation error. Let P_E denote the projector onto the two-dimensional subspace of the (true) noise subspace spanned by $P_N \mathbf{q}_i$. Also, let

$$C_E \equiv \mathbf{G}^H [\mathbf{a}_z, \mathbf{a}_w]^H P_E [\mathbf{a}_z, \mathbf{a}_w] \mathbf{G}.$$

Then, asymptotically, the estimation error is complex circular Gaussian with variance

$$E[\mathbf{v}_\delta \mathbf{v}_\delta^H] \approx \delta \mathbf{G} C_E^{-1} \mathbf{G}^H.$$

Note that $C_E \leq C_N$ (hence $C_N^{-1} \leq C_E^{-1}$) because $P_E \leq P_N$ as positive semi-definite Hermitian matrices. Equality is achieved if the span of \mathbf{q} and the span of $\mathbf{a}_z(z_0, w_0), \mathbf{a}_w(z_0, w_0)$ project onto the same two-dimensional subspace of the noise space.

The variance of the angle estimates is expressed by the 2×2 real matrix $\delta / 2 \Re(C_E^{-1})$. Now,

$$\frac{\delta}{2} (\Re C_N)^{-1} \leq \frac{\delta}{2} \Re C_N^{-1} \leq \frac{\delta}{2} (\Re C_E^{-1}),$$

where the left-hand and right-hand expressions represent the asymptotic error variances of two-dimensional spectral MUSIC and PRIME based on noise-space probes, respectively. It follows that the asymptotic accuracy of two-dimensional MUSIC is generally better. However, for the proper choice of noise-space probes and centrosymmetric planar arrays, the accuracies are identical. In particular, when the array is centrosymmetric and the noise subspace is two-dimensional, the accuracies are identical.



GARY F. HATKE is a staff member in the Advanced Techniques group. His research interests center on adaptive-array processing, with an emphasis on efficient super-resolution algorithms for multidimensional arrays, including polarization-diverse arrays. He also studies performance bounds for adaptive arrays and the application of space-time adaptive processing to multipath interference mitigation.

Gary joined Lincoln Laboratory in 1990, after graduating from Princeton University with a Ph.D. in electrical engineering. He also holds a B.S. degree from the University of Pennsylvania and an M.A. degree from Princeton University, both in electrical engineering. He is an associate editor of *IEEE Transactions on Signal Processing*.